Dermatology

Tattoo and Body Art – Research Article

Dermatology 2023;239:478–493
DOI: 10.1159/000529577

Received: March 7, 2022
Accepted: January 24, 2023
Published online: February 14, 2023

Tattoo Pigments Are Localized Intracellularly in the Epidermis and Dermis of Fresh and Old Tattoos: In vivo Study Using Two-Photon Excited Fluorescence Lifetime Imaging

Marius Kröger Johannes Schleusener Jürgen Lademann Martina C. Meinke
Sora Jung Maxim E. Darvin

Department of Dermatology, Venerology and Allergology, Charité – Universitätsmedizin Berlin, Corporate Member of Freie Universität Berlin and Humboldt-Universität zu Berlin, Berlin, Germany

Keywords
Tattoo · Carbon black particles · Skin · Intravital imaging · FLIM

Abstract
Background: The knowledge about the location and kinetics of tattoo pigments in human skin after application and during the recovery is restricted due to the limitation of in vivo methods for visualizing pigments. Here, the localization and distribution of tattoo ink pigments in freshly and old tattooed human skin during the regeneration of the epidermis and dermis were investigated in vivo. ***Methods:*** Two-photon excited fluorescence lifetime imaging (TPE-FLIM) was used to identify tattoo ink pigments in human skin in vivo down to the reticular dermis. One subject with a freshly applied tattoo and 10 subjects with tattoos applied over 3 years ago were investigated in the epidermal and dermal layers in vivo. One histological slide of tattooed skin was used to localize skin-resident tattoo pigment using light microscopy. ***Results:*** The carbon black particles deposited around the incision have still been visible 84 days after tattoo application, showing delayed recovery of the epidermis. The TPE-FLIM parameters of carbon black tattoo ink pigments were found to be different to all skin components except for melanin. Distinction from melanin in the skin was based on higher fluorescence intensity and agglomerate size. Using TPE-FLIM in vivo tattoo pigment was found in 75% of tattoos applied up to 9 years ago in the epidermis within keratinocytes, dendritic cells, and basal cells and in the dermis within the macrophages, mast cells, and fibroblasts. Loading of highly fluorescent carbon black particles enables in vivo imaging of dendritic cells in the epidermis and fibroblasts in the dermis, which cannot be visualized in native conditions. The collagen I structures showed a higher directionality similar to scar tissue resulting in a greater firmness and decreased elasticity of the tattooed skin. ***Conclusions:*** Here, we show the kinetics and location of carbon black tattoo ink pigment immediately after application for the first time in vivo in human skin. Carbon black particles are located exclusively intracellularly in the skin of fresh and old tattoos. They are found within macrophages, mast cells, and fibroblasts in the dermis and within keratinocytes, dendritic cells, and basal cells in the continuously renewed epidermis even in 9-year-old tattoos in skin showing no inflammation.

Sora Jung and Maxim E. Darvin contributed equally to this work.

karger@karger.com
www.karger.com/drm

Correspondence to:
Maxim E. Darvin, maxim.darvin@protonmail.com
Jürgen Lademann, juergen.lademann@charite.de

Karger

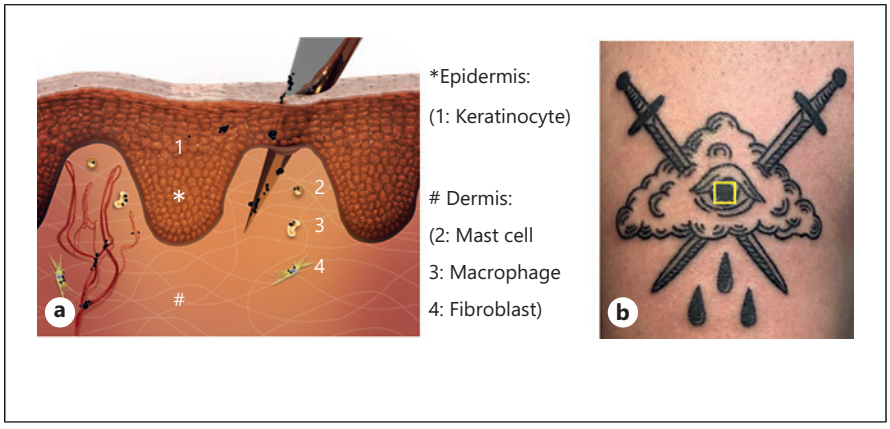

Fig. 1. Schematic illustration of tattoo ink injection into the skin and freshly applied tattoo. **a** The tattoo ink pigments cover the metal micro-needle puncturing the epidermis and the dermis with resident cells, depositing tattoo ink pigments down to approx. 1 mm. The epidermis is labeled *, keratinocytes with 1. The dermis is marked with #, mast cell with 2, macrophage with 3, and fibroblast with 4. **b** A freshly hand-poked tattoo on the thigh with the investigated area of interest (yellow square); the photo was taken immediately after tattoo application. The average depth of the epidermis on the thigh is 70 μm.

Introduction

Skin markings are an old tradition around the globe, with Ötzi the Iceman, the 5,300-year-old Tyrolean mummy, and the Maori in modern-day New Zealand [1]. In a transformation from ritualistic and tribal markings to decorative temporary tattoos, tattooing became ubiquitous and more professional with the development of tattoo machines, reducing application time and manual labor. Scientific research on tattooed skin is mainly focused on the safety [2] and content of tattoo inks [3, 4], as well as the application [5], complications [6], and motivation of tattoo removal [7].

In the European Union, tattoo inks are regulated under Registration, Evaluation, Authorisation and Restriction of Chemicals (REACH) which became effective under the guidance of the European Chemical Agency (ECHA), for the limit concentrations and amounts of hazardous substances, e.g., heavy metals or azo pigments in January 2022, and are about to take effect for pigments blue 15:3 and green 7 in January 2023. The safest tattoo inks are black colored [8], consisting of carbon black due to the chemical inertness of carbon, even though there is a risk of polycyclic aromatic carbohydrates and a carcinogenic risk [9], whereas blue and green inks often contain high concentrations of heavy metals and red inks often contain potentially carcinogenic azo pigments [10]. Høgsberg et al. [3] showed that black tattoo inks are composed of particles of 1–100 nm in size, which may increase their toxicity in the human body. The toxicity of carbon particles is dependent on size, aspect ratio, and surface charge [11], where smaller size and a higher aspect ratio indicate a higher toxicity [12]. The role of dermal injection of particles [13], the effect of particles on fibroblasts [14, 15] and keratinocytes [16, 17], and the dynamics of carbon black particles [18] were investigated previously. While ink particles can lead to, among others, allergic, toxic, and granulomatous skin reactions, their variability in charge, size, and topology as well as the immunomodulatory effects have remained unclear [19, 20]. The investigated carbon black tattoo inks originate from soot and can contain polycyclic aromatic hydrocarbons and benzo(a)pyrene, causing photo toxicity and possibly apoptosis and autophagy in keratinocytes [2].

After insertion into the skin, carbon black particles and their agglomerates can be taken up by macrophages, migrating to perivascular regions (Fig. 1a). Additional processes like pinocytosis [21], which is a form of receptor-mediated endocytosis, where fluids are incorporated into the cell by folding of membrane extrusions, can be involved as a form of cellular nanoparticle incorporation.

Antigen-presenting cells (macrophages, dendritic cells, and B cells) are activated leading to rapid maturation and further infiltration of immune cells into the dermis and epidermis [22–24]; furthermore, antigen-presenting cells initiate a reaction from T cells. From here, the particles can be transported to regional lymph nodes [25], where they remain detectable years after tattooing. Tattoo particles could be even detected in Kupffer cells of the liver indicating a possible hematogenic distribution [26]. Baranska et al. [27] could recently show how tattoo ink pigments are captured and retained dermally by phagocytosis of macrophages, remaining in the cells until the end of their life cycle. Furthermore, dermal fibroblasts which are involved in wound healing, formation of collagen I [28], and phagocytosis [29] are expected to take up tattoo ink pigments up to 2 μm in size [15], at a lower concentration compared to macrophages.

The current understanding is that the epidermis is mostly free of tattoo ink pigments after approximately 4 weeks due to epidermal renewal [30] and clearance of

carbon black particles by keratinocytes, macrophages, as well as regeneration of the dermo-epidermal barrier [31]. Nevertheless, previous histological studies found cases of epidermal carbon tattoo particles in tattoos after 6 months and 7 years of application [32, 33]. Milton and Okun [33] hypothesized that ink particles may be taken up by macrophages, which migrate to the epidermis.

Epidermal ink particles have also been described in a case of chronic photosensitivity and general tattoo reactions to ink particles [34]. Høgsberg et al. [35] described a leakage of red pigment across the dermal-epidermal junction, with transepidermal elimination in 28% of investigated subjects with tattoo reactions. Macrophages and Langerhans cells were commonly found in 95% of biopsies of the dermis and in 47% of the epidermis. Pigments were predominantly engulfed by CD68+ macrophages, and free pigment grains as well as intracellular pigment in Langerhans cells were observed. Transepidermal elimination is a transport process, forming channels from the dermis through the dermal-epidermal junction to the skin surface in order to eliminate exogenous substances from the skin [36–38]. Nickel and chromium from the tattoo needle inserted into the skin have a possible impact on allergic reactions [39].

Pheo- and eumelanins are pigmented biopolymers produced in melanosomes located in melanocytes around the dermal-epidermal junction with a light to dark brown color [40, 41]. In healthy skin, the size of melanosomes and melanin normally does not exceed 500 nm [42], which is smaller compared to carbon black nanoparticle agglomerations, up to several μm in size, as appearing in skin [11] and their concentration strongly decreases from the basal layer of the epidermis with the highest concentration toward the *stratum corneum* (SC) showing the lowest concentration.

Furthermore, induced structural changes and particles' distribution have been described using histological analysis [43], but detailed structural and cellular changes induced by tattooing over time have been missing. Using animal models or excised human skin, many tattoos have been investigated for inflammation, adverse reactions, and poor cosmetic outcome [44], which limits the feasibility of detailed in vivo studies on tattoo particle distribution under physiological conditions. For the first time, tattoo ink pigments in regularly regenerating and healing tattoos are investigated here for their location non-invasively in vivo.

Previous research often relied on biopsies, which are ethically problematic to obtain from newly tattooed asymptomatic human subjects. A method is missing to monitor particle migration in the tattooed skin, to assess the effectiveness of tattoo cosmetics, and to optimize laser tattoo removal. Two-photon excited fluorescence lifetime imaging (TPE-FLIM) [4, 45] is superior in selectiveness and reproducibility compared to single-photon methods [46, 47]. The TPE-FLIM method is capable of non-invasively separating dermal components as recently shown by our group for M1 and M2 macrophages [48], resting and activated mast cells [49], and the main extracellular matrix (ECM) proteins and capillaries of the papillary dermis [49–51] in vivo. Being a non-invasive imaging method, TPE-FLIM enables ethically unproblematic investigations of tattoos on different skin sites.

This study, using TPE-FLIM, focused on the dermal- and epidermal-resident carbon black tattoo ink pigments. First, the TPE-FLIM parameters of carbon black particles were determined in vitro to identify them in human skin biopsies ex vivo. Afterward, the method was transferred to in vivo. A hand-poked tattoo in human skin was used for a case study, where structural changes in tattooed skin were investigated in vivo with tattoo ink pigment location in epidermal and dermal cells over time for 30 months at irregular intervals. Additionally, a cohort study in 10 subjects was conducted, monitoring the epidermal and dermal carbon black nanoparticle distribution and the collagen I fibril directionality.

Materials and Methods

Study Design

At first, the size and aspect ratio of carbon black tattoo ink consisting of carbon black particles (Silverback Ink, Los Angeles, CA, USA) were measured in vitro at a laser power of <1 mW directly on an 18-mm diameter cover glass (VWR, Darmstadt, Germany) at a suspension of 1 μL/mL in PBS. The TPE-FLIM parameters were recorded at the same time at the excitation wavelengths of 735, 760, 775, 790, 805, and 830 nm.

The attenuation spectrum of the carbon black tattoo ink was measured in PBS suspension (60 nL/mL) between 300 and 900 nm in steps of 0.27 nm using a Lambda 650 S UV/VIS spectrometer (PerkinElmer, Waltham, MA, USA). Cultured dermal mast cells isolated from peripheral mononuclear blood cells [52] were exposed to 100 nL/mL carbon black tattoo ink for up to 16 h and measured after 2 and 16 h. Fibroblasts from foreskin were isolated [53] and cultured in a collagen matrix for 24 h and measured as a reference for in vivo investigations.

One 30-year-old subject with skin type II according to the Fitzpatrick classification [54], with pre-existing tattoos, was measured at a recently applied tattoo site (Fig. 1b) on the ventral thigh 14 times, i.e., after 1, 2, 7, 9, 12 days, 3, 4 weeks, and 3, 4, 6, 12, 18, 24, and 30 months after tattooing, from October 2018 to April 2021. Furthermore, 10 additional subjects between 25 and 35 years of age with skin type II-III with tattoos that had been applied at least 3 years ago were measured in vivo at one time point by

TPE-FLIM at the site of their tattoos and in adjacent non-tattooed skin. The tattoos were measured on the volar forearm of 9 subjects and on the calf in 1 subject. Each subject was investigated on at least one tattoo: in 6 subjects, only one tattoo was measured, in 2 subjects two tattoos were measured, and in other 2 subjects three tattoos were investigated. Each tattoo was measured six times per visit in the epidermis and dermis up to a depth of 106 μm. The tattoos were 3, 4, 5, 6, 9, and 10 years old, respectively, and their size ranged between 1 cm × 1 cm and 10 cm × 10 cm. The majority of the tattoos consist of bold black lines with thicknesses between 3 mm and 1 cm. Only in one case, on the 10-year-old tattoo, adverse reactions were self-reported including eczematous skin eruptions that appeared 1 month after tattooing and persisted for 6 months. The residual information about the machine-made old tattoos is summarized in online supplementary Table S1 (for all online suppl. material, see www.karger.com/doi/10.1159/000529577).

The freshly hand-poked tattoo in Figure 1b was located on the thigh. The tattoos in the 10 other subjects were located on the volar forearm and calf, thus on UV-exposed skin sites. A 25-year-old female volunteer of skin type VI without a tattoo was included in the study for melanin control measurements.

TPE-FLIM Tomography

A two-photon tomograph (DermaInspect; JenLab GmbH, Jena, Germany) equipped with a tunable femtosecond Ti:sapphire laser (Mai Tai XF, Spectra Physics, USA, 710–920 nm, 100 fs pulses at a repetition rate of 80 MHz) was used for in vivo imaging of human skin. Under the excitation wavelengths at 760, 795, and 830 nm, a 410–680-nm band-pass filter was used to detect two-photon excited autofluorescence (TPE-AF), and a 375–385-nm filter was used to detect second-harmonic generation (SHG) signals at an excitation wavelength of 760 nm. The lateral and axial resolutions were <0.36 μm and <1.7 μm, respectively [55]. Two-photon excited time-correlated single-photon counting fluorescence lifetime imaging (TPE-FLIM) was processed in the SPCImage software (Becker & Hickl, Berlin, Germany) incorporated into the DermaInspect tomograph. Fluorescence lifetime decay in each pixel was fitted with two exponents (fast and slow decays) with a fixed shift value, and the intensity threshold was chosen depending on the image quality. The obtained lifetime (τ_1 and τ_2) and amplitude (a_1 and a_2) values were further exported and used for the evaluation of lifetime distributions and image segmentation [50]. The mean lifetime was defined as $\tau_m = (a_1\tau_1 + a_2\tau_2)/(a_1 + a_2)$ and further used in the analysis. The instrument response function, whose value is ≈ 80–90 ps, determines the detection limit for TPE-AF lifetimes. In SPCImage (version 8.0; Becker & Hickl, Berlin, Germany), images were processed with an appropriate binning of 3 (square of 49 pixels). The threshold was high enough to block background fluorescence. Relevant parameters were fluorescence lifetimes τ_1 and τ_2, as well as the amplitudes a_1 and a_2.

TPE-FLIM allows a maximal depth of up to approx. 150 μm in non-tattooed skin, which can include the *stratum reticulare* of the lower dermis depending on the skin site and individual skin conditions. The acquisition time was 6.8 s. The utilized two-photon tomography combined with the fluorescence lifetime imaging (TPE-FLIM) system has been previously described in detail elsewhere [49, 56]. Incision size and size of particles were measured through autofluorescence images in the SC.

Skin Biopsy Sections

One skin section of a 15-year-old tattoo was taken from black tattooed skin of a 35-year-old woman after abdominal reduction surgery. Punch biopsies of 6-mm diameter were obtained, snap frozen, and stored at −80°C before cryo-sectioning. Vertical histological cryo-sections of 10-μm thickness were prepared on a cryostat (MICROM cryostat HM 560; MICROM International GmbH, Walldorf, Germany) after embedding in a cryomedium (Tissue Freezing Medium; Leica Biosystems Richmond Inc., Richmond, IL, USA) and placed on 18-mm diameter microscope cover glasses (VWR, Darmstadt, Germany). The anatomical condition of the biopsies was continuously examined using a transmission microscope (Olympus IX 50; Olympus K.K., Shinjuku, Tokyo, Japan). Only high-quality histological sections were used for further analysis. Cell nuclei were stained with Mayers Hematoxylin (Merck, Darmstadt, Germany).

Tattooing Method

The fresh hand-poked tattoo was applied by a professional tattoo artist on the thigh using water-based carbon black tattoo ink (InstaBlack, Silverback Ink, Los Angeles, CA, USA) with a primary nanoparticle size of 50–250 nm, given by the manufacturer. According to the material safety data sheet, the tattoo ink contains the following ingredients and additives: carbon black, CI 77266 as colorant pigment, water as solvent, proprietary alcohol as solvent and regulator of viscosity, proprietary polyvinyl polymer as binding agent, proprietary aliphatic triol as thixotropic agent, proprietary glycol ether as binding agent and humectant, proprietary pyrone acid as preservative. The tattoo needle consists of 18 micro-needles, each of 350 μm in diameter, soldered together in the shape of a circle (Killerink, Liverpool, UK). The length of the taper of the micro-needles is 5.5 mm. The micro-needles are made of 74% steel, 18% chrome, and 8% nickel, known under the specification 304 in AISI nomenclature and 1.4301 in the European EN standard.

In preparation, the area of interest was shaved to avoid insertion of hair into the tattoo and wiped down with 70% ethanol for disinfection. Tattoo ink was injected into the skin up to a depth of approx. 1 mm, as shown schematically in Figure 1a. Carbon black particles were deposited in the skin due to shear forces resulting in a rapidly decreasing viscosity [57] of the tattoo ink; thus, the ink flowed into the skin and stripped off the needle. Overly superficial tattooing can result in a non-saturated and fading tattoo. Tattooing below 2–3 mm within the skin leads to unwanted migration of particles into the capillaries and into the subcutaneous fat, also known as blowout with a typical blue discoloration. Aftercare consisted of the application of a moisturizing ointment twice daily under foil occlusion in order to avoid dryness and to keep the scab and skin flexible.

The older tattoos in the ten other volunteers were machine-made by professional tattoo artists using a tattoo needle (with 1–15 micro-needles) penetrating deeper into the skin than a hand-poked tattoo, with a frequency of up to 3,000 times per minute with unknown carbon black-based tattoo inks. The tattoos in these 10 subjects were at least 3 years old. Aftercare included the same procedures as described above. None of the tattoos, except for the freshly applied tattoo, showed clinical or subjective signs of inflammation, adverse reactions, or other side effects.

Skin Elasticity

The skin elasticity was measured using the Cutometer® MPA580 (Courage Khazaka, Cologne, Germany). A negative pressure was applied to a 2 mm × 2 mm area of the skin for 2 s, returned to normal pressure, and repeated for 10 times in each skin spot. Utilizing an optical method, the displacement of the skin was measured. The resulting parameters were calculated for firmness and elasticity of the skin: R_{firmness} describing the amplitude of displacement with lower values indicating firmer skin, lower values indicating a higher firmness, and $R_{\text{elasticity}}$ describing the relation between the maximum of the amplitude to the degree of back formation with higher values indicating a higher elasticity. Each measurement was performed three times in the tattooed skin and three times in non-tattooed skin in close proximity.

Directionality of Altered ECM

Changes in the dermal ECM, especially collagen I structures, were measured by directionality as an indicator of skin alteration [51, 58]. The alteration of collagen I structures was processed by the SHG images, following binarization of the image. A fast Fourier transformation was performed, and the result was fitted to an ellipse consisting of the short axis a and the long axis b. The directionality parameter d was calculated as $d = a/b$, with a higher value of d indicating a higher directionality.

Statistical Analysis

TPE-FLIM data for all dermal components were recorded, descriptive statistics were applied, and directionality processed using MATLAB R2020b (MathWorks, Natick, MA, USA). All values were presented as mean ± standard deviation.

Results

Determination of TPE-FLIM Parameters of Carbon Black Particles in vitro

Carbon black particles are fluorescent active. It was observed that the additives in the tattoo ink, listed in the materials section, showed no or negligible fluorescence; thus, only the carbon black particles are responsible for the fluorescence signal. In order to detect carbon black particles in human skin, first their TPE-FLIM parameters were determined in vitro. TPE-FLIM lifetimes were τ_1 = 108 ± 25 ps at a_1 = 96%, τ_2 = 800 ± 100 ps at a_2 = 4%, and τ_m = 125 ± 50 ps, with wavelength independence between 735 and 830 nm (data not shown). The average size of carbon black particle aggregates in PBS was 500 ± 150 nm measured using the TPE-FLIM method. Smaller carbon black particles can be detected as blurry spots with the characteristic TPE-FLIM parameters. The one-photon excited attenuation spectrum of the carbon black was measured as a suspension in PBS. As expected and according to aggregate size, the attenuation decreased from ≈0.46 at 300 nm to ≈0.15 at 900 nm, which is shown in online supplementary Figure S1.

TPE-FLIM parameters of carbon black particles are shown in online supplementary Table S2 compared to dermal cells. The fluorescence lifetimes of carbon black are close to the instrument response function. The dermal cells present significantly different TPE-FLIM parameters and, thus, can be distinguished in the skin.

Carbon Black and Melanin ex vivo and in vivo

A cryo-biopsy of tattooed abdominal skin (tattooed 15 years ago) of a 37-year-old female was measured to establish a baseline of carbon black particle distribution in fully recovered skin after tattooing. Carbon black particles are found exclusively inside the cells close to the cell nuclei (Fig. 2a) and within the cell agglomerations (Fig. 2b) in the dermis, which are marked with green arrows in the dermis (Fig. 2). Melanin in the epidermis is gray translucent, due to the light skin color of the subject, marked with an orange ellipse in Figure 2 in the *stratum basale* (SB). On rare occasions, carbon black agglomerates are seen in the epidermis as black spots (yellow circle). The agglomerations of carbon black are significantly larger with a higher fluorescence intensity and contrast compared to melanin in the SB (Fig. 2b).

To identify the carbon black particle distribution in the skin in vivo, tattooed skin of one subject of Fitzpatrick skin type II, with an old hand-poked tattoo applied 18 months ago (Fig. 1b), was scanned from the SC toward the papillary/reticular dermis (depth 75–90 μm) with 20–50 mW laser power and excited between 735 and 830 nm using TPE-FLIM. The TPE-FLIM parameters of carbon black were found to be the same as determined in vitro and wavelength and time invariant. The TPE-FLIM parameters of the skin components however were dependent on wavelength, with shorter fluorescence lifetimes toward longer excitation wavelengths. Additionally, the excitation wavelength at 760 nm allowed to visualize collagen I in a separate channel at 380 nm due to the appropriated contrast of skin structures and high quality of the recorded images; see online supplementary Figure S2.

The fluorescence intensity of carbon black particles in this subject is 2.75 times higher with 4,125 photons/mW compared to 1,500 photons/mW in the melanin-rich SB. The size of melanin granules was below the detection limit of the two-photon tomograph, yet the melanin was visualized as FLIM-lifetime overlay indicating short fluorescence lifetimes in red (online suppl. Fig. S3). In the keratinocytes in non-tattooed skin of a volunteer with skin type II, melanin was visible, while parts of the non-tattooed skin of type VI were similar in appearance to the tattooed skin type II (online suppl. Fig. S2a, c).

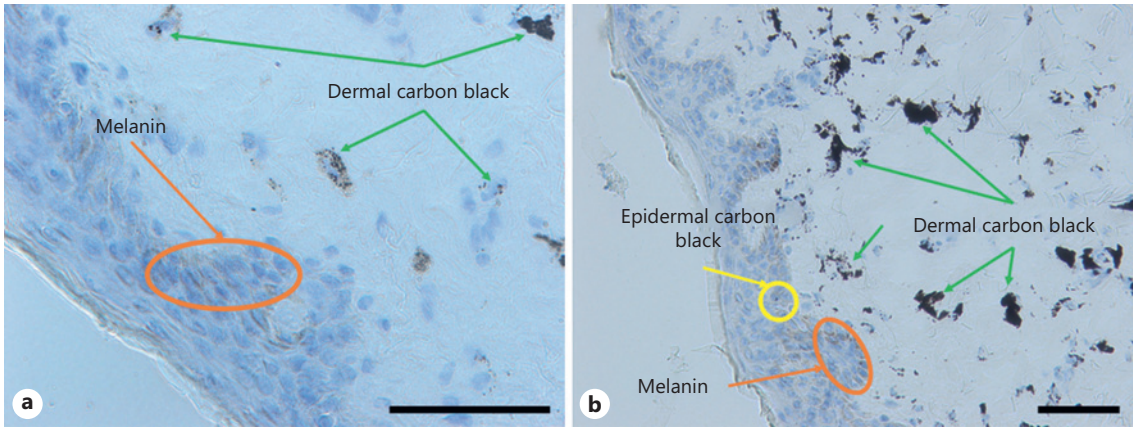

Fig. 2. Biopsy section of 15-year tattooed human abdominal skin of 37 y.o. woman. Representative light field microscopic images of tattooed skin: blue – the cell nuclei; black – the carbon black nanoparticles; gray translucent – melanin. Carbon black nanoparticles are located exclusively in the cells (green arrows) in close proximity to the nuclei (**a**) and in cell agglomerations with carbon black nanoparticles in the epidermis, marked with a yellow circle (**b**). Melanin in the *stratum basale* is marked with an orange oval. Cell nuclei were stained with Mayers Hematoxylin. Scale bar for all images is 50 μm.

Regeneration of Tattoo Needle-Induced Skin Incisions in Hand-Poked Tattoo

The skin healing progress of needle-induced damage of one hand-poked tattoo was investigated at different time points, and the TPE-AF image of incision holes is shown in Figure 3. The incision size decreased over time from an average of 60 ± 30 μm at day 1 after application (Fig. 3a) to 10 ± 5 μm at day 84 post-application (Fig. 3b–d) decreasing in size thereafter. Epidermal and dermal damage caused by the incisions of the 350 μm microneedle is expected to fully recover following application. In Figure 3d–f, the carbon black particle agglomerates are clearly visible inside the keratinocytes of the *stratum spinosum* (SSp), sometimes even reaching up to the SC for months after application. The size of carbon black agglomerations over time is shown in online supplementary Figure S4, where the agglomerates of 1.5 ± 0.9 μm at day 1 increased in size up to 7.2 ± 0.7 μm at approx. 100 days and then decreased, partially retrieved from Figures 3 and 4.

Epidermal-Resident Carbon Black Particles in Hand-Poked and Old Machine-Made Tattoos

After initial skin regeneration, the epidermis of the hand-poked carbon black tattoo (Fig. 1b) was measured during 30 months to investigate the distribution of carbon black particles in the clinically fully regenerated tattooed skin. Carbon black nanoparticle agglomerates were visible in all layers of the epidermis after 30 months (Fig. 4; online suppl. Fig. S5c, d). As shown in Figure 4a and online supplementary Fig. S8 (6 years old), the TPE-FLIM intensity of carbon black agglomerates is significantly higher compared to cellular epidermal structures, while TPE-AF lifetime is significantly shorter compared to the corneocytes of native SC (Fig. 4a, b), *stratum granulosum* (Fig. 4c, d), and SSp (Fig. 4e, f).

Here, small carbon black particle agglomerates were observed inside the keratinocytes. In Figure 4g and h, an epidermal carbon black-loaded suspected dendritic cell in the SSp in tattooed skin is shown with fluorescence lifetimes τ_1 = 100 ± 5 ps, τ_2 = 1,299 ± 60 ps, and τ_m = 141 ± 15 ps, clearly distinguishable from the keratinocytes by its dendritic appearance. In the SB, carbon black particles with TPT-AF lifetimes τ_1 = 95 ± 5 ps, τ_2 = 1,161 ± 50 ps, and τ_m = 136 ± 20 ps could be observed by their high TPE-AF intensity (online suppl. Fig. S5a), as melanin located in melanocytes masked the TPE-FLIM parameters of the carbon black particles due to slightly longer lifetimes (Fig. 4j) τ_1 = 121 ± 10 ps, τ_2 = 1,524 ± 50 ps, and τ_m = 181 ± 10 ps. Using the FLIM method, melanin could only be observed as a homogeneous area without visualization of the melanosome substructures. The size of carbon black nanoparticle agglomerates in epidermal cells was smaller than 4 μm (Fig. 4). No carbon black particles were observed in the intercellular space of the epidermis 3 weeks after the application.

Furthermore, 16 machine-made carbon black tattoos, which were applied at least 3 years ago, were investigated in the skin of 10 subjects. Although the tattooed skin sites had regenerated without any clinical sign of inflammation or adverse reaction to the ink, carbon black particle agglomerates could be detected in epidermal cells in 8 of

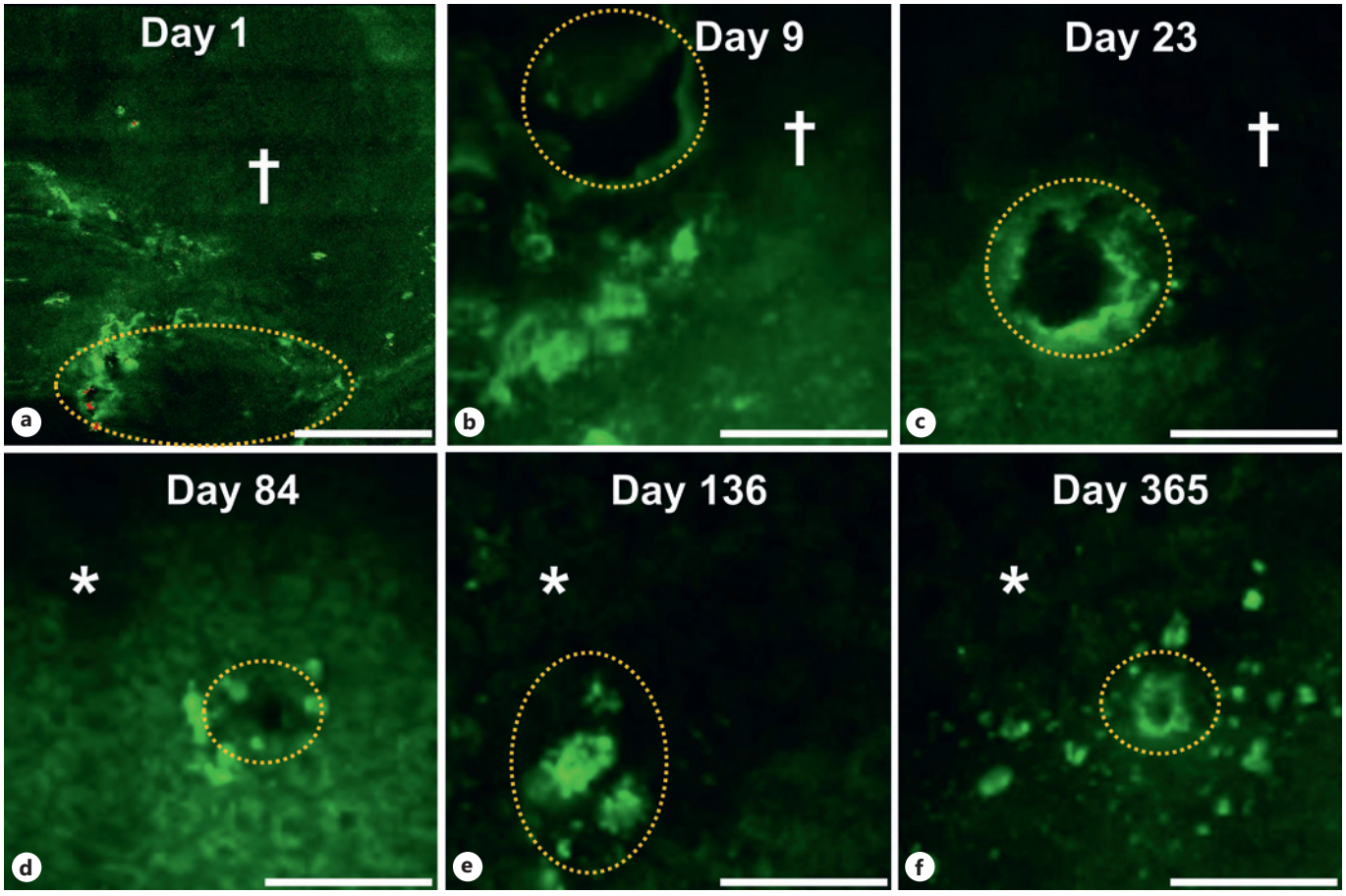

Fig. 3. Time dynamics of skin micro-needle incisions (dotted oval) after application. Representative TPE-AF image of incision holes (**a–f**) and surrounding keratinocytes (**d–f**) and carbon black tattoo ink pigments measured consecutively after tattoo application in one volunteer (Fig. 1b) on day 1 (**a**), depth 10 µm, day 9 (**b**), day 23 (**c**), day 84 (**d**), day 136 (**e**), and day 365 (**f**). † marks images acquired in the *stratum corneum*, * marks images in the SSp. Carbon black nanoparticles are visible as bright white spots around the incisions. All images were acquired using TPE-FLIM at 20 mW, 760 nm, and 6.8 s acquisition time at a depth of 35–50 µm (**b–f**). Scale bar for all images is 30 µm.

10 subjects several years after application. While 12 of 16 (75%) individual tattoos showed tattoo ink particles in epidermal cells, in other tattoos of the same subjects, no carbon black particles were detected within the epidermis.

Carbon black particle agglomerates were still observable in the epidermis of a 3-year-old machine-made tattoo on the volar forearm, as shown in online supplementary Figure S3c, with fluorescence lifetimes τ_1 = 105 ± 5 ps, τ_2 = 1,430 ± 80 ps, and τ_m = 125 ± 10 ps. The size of the particle agglomerates does not exceed 4 µm. In the SB, the carbon black tattoo pigments were distinguishable from melanin by higher TPE-AF intensity and distinct, point-like morphology, and slightly longer TPE-AF lifetimes in Fitzpatrick skin type II. Melanocytes were clearly observed at 52 µm depth in a subject of skin type II without tattoos (online suppl. Fig. S3d), a non-tattooed subject with skin type VI (online suppl. Fig. S3e), and at 55 µm depth in the tattooed subject of skin type II (online suppl. Fig. S3f). While carbon black particles could be detected within epidermal cells as bright short lifetime spots inside epidermal cells, for up to 9 years after application (online suppl. Fig. S5a, b), a decrease in intracellular ink pigment density was observed.

Carbon Black Nanoparticle Distribution in Dermal Cells in Hand-Poked Tattoo and Older, Machine-Made Tattoos

In the dermis, carbon black particle agglomerates were detected in TPE-FLIM images as bright red spots located exclusively inside the cells – macrophages (Fig. 5a, b), mast cells (Fig. 5c, d), and fibroblasts (Fig. 5e–h), characterized by the short fluorescence lifetime and in the

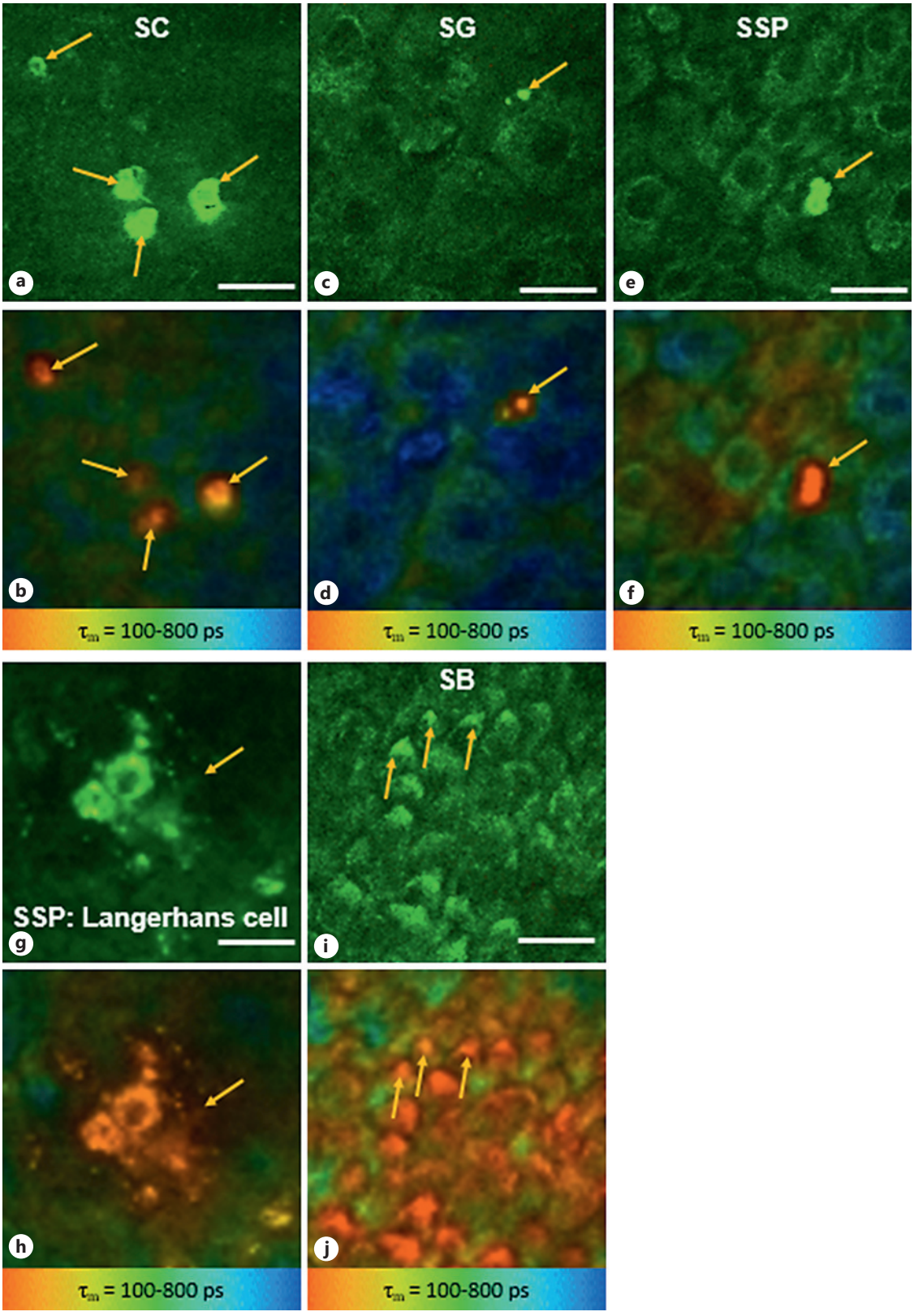

4

(For legend see next page.)

TPE-AF images by their intense TPE-AF intensity, as presented in Figure 5 as bright fluorescent green areas inside the fibroblasts. Identification of dermal cells by their morphology, location, and the specific TPE-FLIM parameters was described elsewhere by our group [48, 49].

M1 macrophages (Fig. 5b; online suppl. Fig S6c) were 10–18 μm in dimension, of an irregular shape, and had an exceptionally high TPE-FLIM intensity of 1,900 photons/mW at 82 μm depth with fluorescence lifetimes $\tau_1 = 100 \pm 5$ ps, $\tau_2 = 1{,}150 \pm 50$ ps, and $\tau_m = 122 \pm 10$ ps. Only around half of the usual laser power was required (approx. 28 mW) to achieve the same photon density at this depth compared to non-tattooed skin, which indicates the presence of highly fluorescent carbon black particles inside the macrophages. The cross section of the M1 macrophage with a high TPE-AF intensity is presented in Figure 5b, showing short TPE-AF lifetimes, which is typically indicative for phagocytosing M1 macrophages [59].

Carbon black particles could be detected in perivascular mast cells (Fig. 5c, d). The mast cell located in the papillae extends vertically into the papillary dermis, with an oblong shape, a length of ≈10 μm and unusually short fluorescence lifetimes of $\tau_1 = 109 \pm 7$ ps, $\tau_2 = 1{,}826 \pm 80$ ps, and $\tau_m = 139 \pm 15$ ps in vivo, compared to $\tau_1 = 83 \pm 2$ ps, $\tau_2 = 1{,}066 \pm 55$ ps, and $\tau_m = 136 \pm 10$ ps in vitro (online suppl. Fig. S7), which is comparable to carbon black particles. The mast cell in Figure 5d showed the same morphology and shorter TPE-AF lifetime compared to an activated mast cell in non-tattooed skin, which is in accordance with recently published data for dermal mast cells in vivo [49].

In Figure 5e–h, suspected fibroblasts, which absorbed the carbon black tattoo pigment, are shown at 74 μm depth inside a dermal papilla with fluorescence lifetimes $\tau_1 = 100 \pm 5$ ps, $\tau_2 = 1{,}462 \pm 50$ ps, and $\tau_m = 127 \pm 12$ ps. The fibroblasts have a visible cross section of max. 15 μm and a lower TPE-AF lifetime compared to the ECM, which is due to the presence of carbon black particles. The size and shape are similar to dermal fibroblasts measured in vitro and shown in online supplementary Figure S8. In Figure 5e–h, fibroblasts, densely located in the papillary dermis, were observed in the tattooed skin in vivo using TPE-AF. The carbon black particles were homogeneously distributed inside the fibroblasts, resulting in highly dendritically shaped fluorescence intensity spots. All TPE-FLIM parameters agree with the parameters of carbon black particles.

Structural Changes in the Dermal ECM in Tattooed Skin in Older, Machine-Made Tattoos

Changes in the ECM can be assessed by changes in elasticity and stiffness of the skin. The subjects themselves reported no subjective difference in skin stiffness and elasticity for tattooed and non-tattooed skin. In vivo measurements of the skin elasticity with the cutometer revealed a significantly increased ($p < 0.05$) mean firmness in tattooed skin of 0.27 ± 0.04 arb. units compared to non-tattooed skin with 0.34 ± 0.04 arb. units. Skin elasticity was shown to have decreased in tattooed skin (0.78 ± 0.09 arb. units) compared to non-tattooed skin (0.88 ± 0.07 arb. units), $p < 0.05$, and the changes in the ECM are visible using SHG imaging of collagen I. The collagen I fibrils are on average 47 ± 5% thicker in tattooed skin, exhibit a higher directionality, and are less interwoven (Fig. 6a) compared to non-tattooed control (Fig. 6b). A Fourier analysis regarding the directionality of collagen I fibrils revealed a directionality value of $d = 0.87 \pm 0.09$ in tattooed skin and $d = 0.96 \pm 0.04$ in non-tattooed skin, where a value of 1 shows no directionality. The differences were found to be statistically significant ($p < 0.05$).

Discussion

The fluorescence lifetime of carbon black is short, is close to the instrument response function (≈90 ps), has an

Fig. 4. In vivo distribution of carbon black tattoo nanoparticles in the epidermis of healed hand-poked tattoo after 30 months. TPE-AF images (**a**, **c**, **e**, **g**, **i**) and corresponding TPE-FLIM images (**b**, **d**, **f**, **h**, **j**) of skin tattooed with carbon black nanoparticles of a 30-month old tattoo on the thigh at 10 μm depth in the *stratum corneum* (SC) with fluorescence lifetimes $\tau_1 = 104 \pm 5$ ps, $\tau_2 = 578 \pm 20$ ps, and $\tau_m = 136 \pm 12$ ps (**a**, **b**), at 22 μm depth in the *stratum granulosum* (SG) with fluorescence lifetimes $\tau_1 = 101 \pm 7$ ps, $\tau_2 = 1{,}112 \pm 50$ ps, and $\tau_m = 151 \pm 10$ ps (**c**, **d**), at 35 μm depth in the *stratum spinosum* (SSp) with fluorescence lifetimes $\tau_1 = 107 \pm 5$ ps, $\tau_2 = 1{,}453 \pm 30$ ps, and $\tau_m = 148 \pm 10$ ps (**e**, **f**), and TPE-FLIM image of tattooed skin of a tattoo applied 6 months ago at a depth of 42 μm showing a suspected carbon black-loaded dendritic cell (arrow) with fluorescence lifetimes $\tau_1 = 100 \pm 5$ ps, $\tau_2 = 1{,}299 \pm 60$ ps, and $\tau_m = 141 \pm 15$ ps (**g**, **h**) and at 48 μm depth in the *stratum basale* (SB) with fluorescence lifetimes $\tau_1 = 95 \pm 5$ ps, $\tau_2 = 1{,}161 \pm 50$ ps, and $\tau_m = 136 \pm 20$ ps (**i**, **j**). Most of the bright red-orange structures in **j** are melanin in basal cell with fluorescence lifetimes $\tau_1 = 121 \pm 10$ ps, $\tau_2 = 1{,}524 \pm 50$ ps, and $\tau_m = 181 \pm 10$ ps, and the arrow-depicted red-orange dots are carbon black. Carbon black particles, marked with arrows, are visible inside epidermal cells by their strong fluorescence intensity (**a**, **c**, **e**, **g**, **i**) and short fluorescence lifetime (**b**, **d**, **f**, **h**, **j**). The images are recorded at 24 mW, 760 nm excitation, and 6.8 s acquisition time. The scale bar is 12 μm.

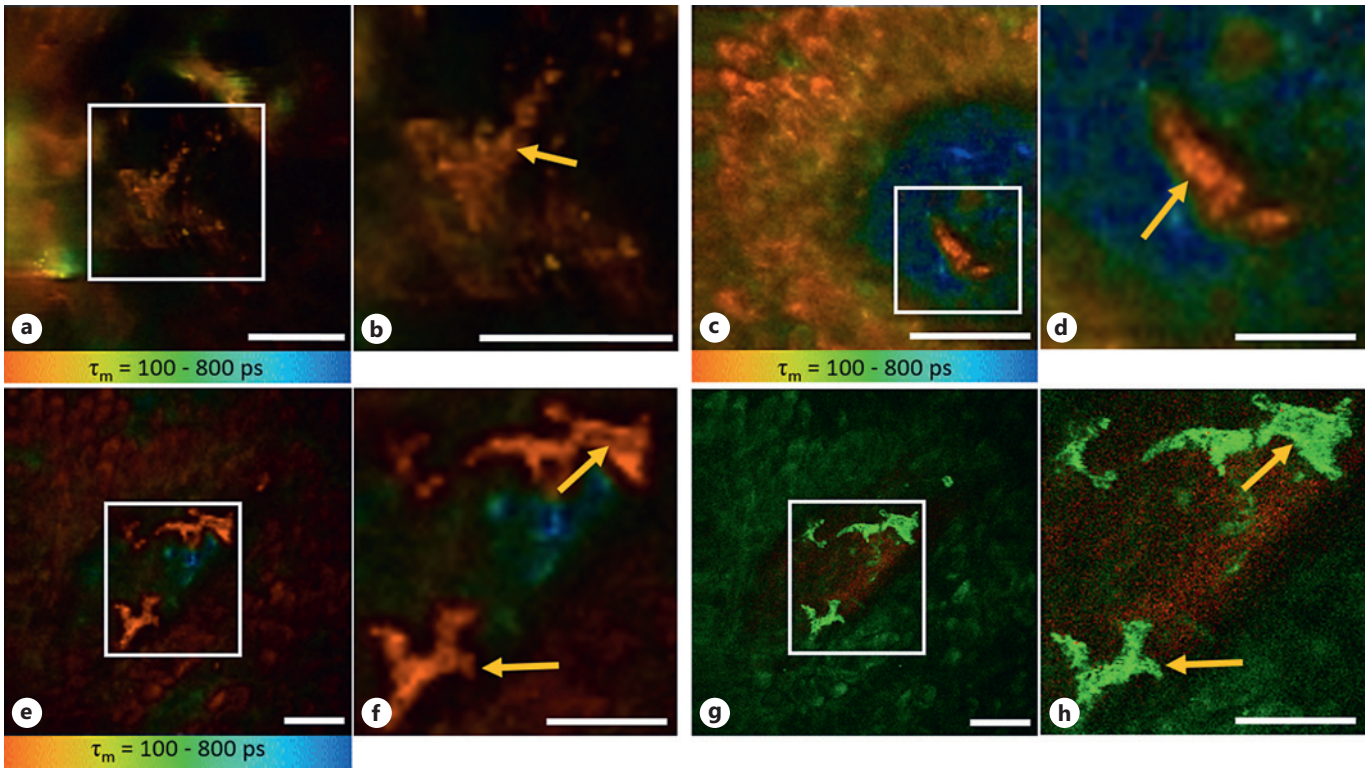

Fig. 5. TPE-FLIM images of human dermal immune cells in tattooed skin in vivo. Full size images (**a**, **c**, **e**, **g**) and 100% larger zoomed details of the white squares (**b**, **d**, **f**, **h**). TPE-FLIM images of the M1 macrophage (square) phagocyting carbon black nanoparticles (bright red areas, shown with an arrow (**b**)) in the marked cell at 82 µm depth in a 3-year-old tattoo with fluorescence lifetimes τ_1 = 100 ± 5 ps, τ_2 = 1,150 ± 50 ps, and τ_m = 122 ± 10 ps (**a**, **b**); a perivascular activated mast cell (square) containing carbon black nanoparticles (arrow (**d**)) at 85 µm depth of an 18-month old tattoo with fluorescence lifetimes τ_1 = 109 ± 7 ps, τ_2 = 1,826 ± 80 ps, and τ_m = 139 ± 15 ps (**c**, **d**); dermal carbon black nanoparticle-loaded (arrow (**f**)) fibroblasts (square) at 74 µm depth in a 30-month old tattoo with fluorescence lifetimes τ_1 = 100 ± 5 ps, τ_2 = 1,462 ± 50 ps, and τ_m = 127 ± 12 ps (**e**, **f**); TPE-AF (green) and SHG (collagen I, red) of carbon black nanoparticle-loaded fibroblasts (bright green, marked with square) surrounded by basal cells (dim green), with collagen (red) in between the fibroblasts of a 30-month old tattoo (**g**, **h**). Images were acquired using TPE-FLIM, TPE-AF, and SHG at 28 mW, 760 nm excitation, and 6.8 s acquisition time. Scale bar is 10 µm.

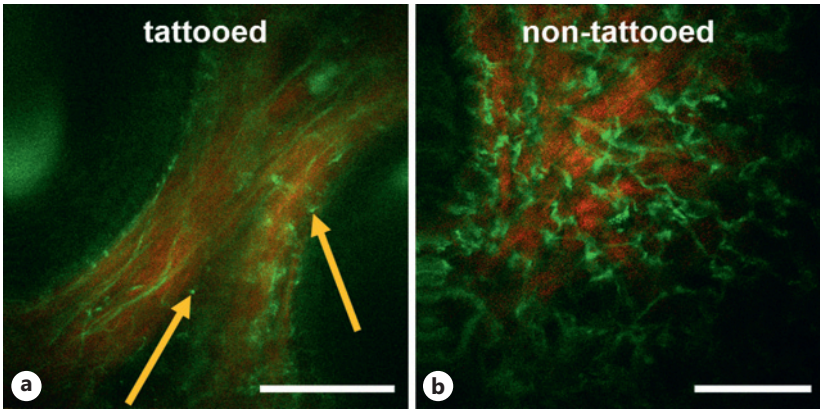

Fig. 6. Collagen I structures in tattooed and non-tattooed skin. TPE-AF (displaying elastin and carbon black particles as green structures) and SHG image (showing collagen I as red structure) as composite for tattooed skin (**a**) and non-tattooed skin (**b**). The tattooed skin shows thicker fibrils and a higher directionality with carbon black particles signified by orange arrows. Images were acquired at 35 mW at 760 nm and 90 µm depth using TPE-FLIM. Scale bar for all images is 30 µm.

almost mono-exponential decay, and is independent of the excitation wavelength (735–830 nm). The TPE-FLIM parameters of carbon black particles are similar to melanin [60]; however, the TPE-AF intensity is higher for carbon black.

The TPE-FLIM signatures of the ECM and dermal cells [48, 49], shown in online supplementary Table S2, are not superimposed by fluorescence lifetime of carbon black nanoparticles excited at 760 nm. Carbon black particles can be separated from melanin-containing melanosomes by the granular-like inhomogeneous appearance in the FLIM image (Fig. 4), the larger size of the carbon black agglomerates in cells (Fig. 2), which is not specific for melanin [61], and the highest TPE-AF intensity (online suppl. Fig. S2b). While carbon black particles tend to agglomerate, melanosomes show a higher mobility and do not trigger phagocytic abilities in epidermal cells. Carbon black particles tend to aggregate into larger sizes compared to the size of melanin granules [40] as shown in Figures 2 and 4. Melanin and carbon black particles below the resolution threshold can be detected as blurry spots and can be seen in the SB in Figure 4j and online supplementary Figure S3b. The short fluorescence lifetime of basal cells is solely due to the incorporated melanin. The TPE-FLIM lifetimes of carbon black are constant and are independent of the concentration due to the bigger size of the agglomerates in contrast to melanin where the lifetime depends on the concentration. In Fitzpatrick type II skin, the basal cells have a longer lifetime compared to carbon black, whereas in Fitzpatrick type VI skin the lifetime of melanin-loaded basal cells is shorter compared to carbon black. Thus, carbon black particles that are smaller than the resolution of the TPT can be visualized as short fluorescence lifetime overlay on cells and ECM, and the study is limited to skin types I and II.

Tattooed skin is expected to have clinically regenerated when erythema, scaling, and itch subsided, and the skin is smooth. These clinical criteria were observed in the hand poke-tattooed subject 3 weeks after application and in all tattooed subjects at the time point of each measurement. The duration of recovery of needle-caused incisions below the SC can be longer [31] than the usual epidermal recovery time upon visual inspection of 3–4 weeks after tattooing (Fig. 3). Epidermal irregularities such as smaller gaps between keratinocytes had still been visible 84 days after tattoo application, when the regeneration of the dermal-epidermal junction was completed and the tattooed subjects perceived the tattooed skin as clinically fully healed. It remains unclear whether the explanation for this phenomenon is interstitial fluid between keratinocytes and apoptotic keratinocytes, or whether the non-fluorescent spot is the nucleus of a carbon black containing epidermal cell (Fig. 3).

Epidermal cells are identified by their morphological features, the depth they are found in and their appearance, which has been reported in literature [62]. As cellular structures are not visible in the microscopic images of the SC (Fig. 4a, b), it is not clear whether the carbon black agglomerates were inside or between the corneocytes. The size of carbon black agglomerates in the SC is larger compared to those in the *stratum granulosum* and SSp. It may be possible that carbon black agglomerates distributed in the keratinocytes are fused in the flattened corneocytes or within the extracellular lipid matrix around them. The observation of the structural changes directly after tattoo application in vivo is limited to a single subject in our investigations, where no clinical adverse reactions to the tattoo ink were observed.

Suspected dendritic cells (Fig. 4g, h) filled with carbon black particles were identified by their dendritic appearance in the epidermis, similar to labeled fluorescence microscopy studies [63, 64] and the proven ability to execute phagocytosis [65] – of carbon black particles in our case. Only two dendritic cells were clearly identified in the present study. Future studies should address further characterization and the density of dendritic cells. Dendritic cells are able to cross the epidermal to dermal tight junction, opening a pathway for particle transport into the epidermis.

Carbon black particles were observed in the epidermis in machine-made tattoos. Høgsberg et al. [35] described a leakage of red pigment across the dermal-epidermal junction into the epidermis in 28% of investigated subjects, while in the presented study, 75% of the tattoos exhibited epidermal ink (online suppl. Fig. S3, S5). In this study, no carbon black particles were observed in the intercellular space in the epidermis (Fig. 4; online suppl. Fig. S3, S5). Høgsberg et al. showed the transepidermal transport in red tattoos which give significantly different immune responses. Presumably, the red inks have a higher allergic potential, since allergic tattoo reactions can be seen especially to red tattoo ink depending on its components [66, 67]. This can lead to an increased transport out of the epidermis and that could be why our workgroup could see epidermal ink pigments in more subjects.

Carbon black particles are likely to be found directly after injection in intra- and extracellular compartments of the epidermis, but it is unlikely for carbon black particles under physiological conditions to be retained several months after regeneration of the epidermis. Taylor et al.

[32] found pigments in the epidermis with a histologically intact dermal-epidermal barrier, even though the findings were rare, due to a lower popularity and prevalence of tattoos in the early 1990s. The amount of tattoo ink pigment in the epidermis of old tattoos depends on lifestyle parameters such as UV exposure. Male subjects showed a higher prevalence of tattoos, working more often outdoors, while the awareness for sun protection was less prevalent in the general population [68, 69].

A possible pathway of particles through the base membrane of variable permeability can occur when the skin is exposed to irritants [24, 70] or the skin is exposed to UV light [23, 71, 72]. In these cases, monoclonal monocytes and dendritic cells are infiltrating the dermis and epidermis, following the production of cytokines IL-6, IL-8, TNF-α, and have the potential to differentiate to cd11+ dendritic cells and Langerhans cells in the epidermis and dendritic cells and macrophages in the dermis. Other dendritic cells are replacing depleted Langerhans cells. This infiltration may happen without the subject noticing clinical symptoms. It is hypothesized that monocytes on their path to the epidermis transport carbon black particles from the dermis, due to the phagocytic abilities of monocytes [73], although the phagocytic ability varies significantly between subjects according to Gu et al. [74] which could explain the absence of ink pigment in some subjects.

If the particles are located within the epidermis, we expect at least two different processes to release particles via the epidermis: the first process is well known, via epidermal regeneration or turnover. Nevertheless, infiltration of phagocytically active cells into the epidermis increases retention time of carbon black particles, due to the dendrites capturing the particles. On the other hand, due to inflammatory responses in keratinocytes, similar to fine dust [75] the particles can induce an inflammatory response, and in conjunction with the increased energy transmission from sun light into the keratinocytes of highly scattering carbon black particles, the viability of keratinocytes is significantly reduced promoting the depletion of tattoo pigments from the epidermis as seen in old tattoos on subjects with high UV exposure.

Currently, no data are available for quantification of particle transport between the epidermis and the dermis, because methods to measure particle transport in vivo are missing. The new TPT method can help estimate the amount of transported particles in future studies.

Dermal cells in the papillary dermis in 70–95 μm depth were found to absorb carbon black particles intracellularly (Fig. 5) which is in accordance with published data [15, 27, 35, 76]. It can be assumed that carbon black particles, just as shown for other particles, are also taken up by cells as a result of pinocytosis and endocytosis. The uptake and storage of ink particles into fibroblasts, dendritic cells, and macrophages have been shown previously [77, 78]. The exact mechanisms of uptake were not part of these investigations, but could be the focus of further studies. Ferguson et al. [76] conducted ex vivo measurements with a more aged cohort and older tattoos, in a time when tattooing was less professionalized and tattoo inks had higher limits for toxic and carcinogenic substances, such as heavy metals and irritants. Strandt et al. [15] showed concentrations of tattoo inks in the cells isolated from mice tail skin. These mice cannot be compared to humans, as the immune system is different from a human compared to a mouse living in pathogen-free conditions. Additionally, a green phthalocyanine pigment was used and further investigations have to show if the pigment is handled by the dermal cells comparably to carbon black.

In vivo identification and classification of mast cells [49] and macrophages [48] were shown by our workgroup using TPE-FLIM, compared in online supplementary Table S2 [48]. Fibroblasts can be identified by morphologic features, highly dendritic features (online suppl. Fig. S8c), their location, and the fact that they are known to show phagocytic activity in tattoos [15, 79]. In non-tattooed skin, fibroblasts are not detectable by the TPE-FLIM method as the TPE-AF intensity is lower compared to the TPE-AF intensity of other dermal components [49], due to a low metabolic activity in NAD(P)H and low concentration of reactive oxygen species [80]. The detection capacity of the TPE-FLIM method reaching into the reticular dermis, down to 106 μm in tattooed skin, simultaneously visualizing dermal cells loaded with carbon black nanoparticles and ECM in the form of elastin is shown in online supplementary Figure S6 for the 6-year-old tattoo. The influence on collagen I synthesis of carbon black-loaded fibroblasts remains unclear [29].

Collagen I and elastin structures in tattooed skin were expected to change similar to a wound healing process [81]. The results of this pilot study with a limited number of volunteers suggest a significant change in collagen I structure of the dermis caused by the tattoo application. The dermal ECM and collagen I structures close to tattoo pigment-containing dermal cells are observed to have a higher directionality and increased fibril diameter, as known from histological examinations of scar tissue [28] and skin atrophy [82]. These results are supported by the observation of increased skin firmness and decreased skin elasticity in tattooed skin and are consistent with the

observation of (47 ± 5) % thicker collagen I fibrils in tattooed skin with more directed and less interwoven fibers with an increase of collagen mass, which presumably leads to a stiffer and less elastic skin (Fig. 6). Dermal collagen I in asymptomatic non-tattooed young skin was assumed to have no significant directionality. Grant et al. [29], analyzing biopsies, have also reported a more parallel organization and a higher directionality of dermal fibrillary collagen I and III in tattooed skin, confirming our results.

The lateral detection limit is <0.36 μm with slight increase in the dermis, due to scattering. Therefore, that part of such pigment particles, especially if present in non-agglomerated form, will appear as blurry spots and overlays with a short fluorescence lifetime of approx. 100 ps on cellular and extra cellular structures with otherwise differing TPE-FLIM signatures. However, this did not affect the purpose of this study to show the distribution and agglomeration of the tattoo ink pigments in the epidermis and dermis. A limitation of the study was that incisions could only be measured in the epidermis, due to the high epidermal carbon nanoparticle load early after tattoo application and subsequent highly absorbing and scattering optical properties. In general, tattoos on the forearm facilitate a deeper penetration into the dermis, because of greater environmental UV exposure. Skin sites that are usually covered showed a higher pigment density and a lower penetration depth of excitation light around 70–80 μm. Furthermore, the motif of the tattoo is critical where a full black area shows a higher pigment density [83] compared to a motif consisting of multiple thin lines. In online supplementary Figure S6, different areas were shown regarding the visibility of the dermal layer in 106 μm in the reticular dermis, showing co-visualization of cellular incorporated carbon black particles and ECM.

Conclusions

This in vivo study showed the distribution of tattoo particles and structural changes in human skin using TPE-FLIM for the first time. Carbon black particles can occasionally be detected intracellularly within the epidermis even after 9 years. A small concentration of carbon black particles was found in the epidermal cells – keratinocytes and dendritic cells, which indicates the continuous release of small amounts of tattoo ink particles from the dermis toward the epidermis. The results of the present in vivo study in humans indicate that in fully recovered tattooed skin, carbon black particles are resident mainly in dermal cells. Herewith, dermal fibroblasts, M1 macrophages, and mast cells serve as contributors to particle storage, in the absence of carbon black particles in the ECM. Collagen I structures around ink deposition sites containing fibroblasts change comparable to scarring. Collagen I fibrils in the tattooed skin have a higher directionality, are less interwoven, and are thicker, which results in an increase in skin stiffness and decrease of skin elasticity.

Key Message

Tattoo pigments are localized intracellularly in the epidermis and dermis.

Acknowledgments

We thank David Satzinger for the tattoo illustration, Benjamin Greif for design and application of the tattoo and providing tattoo ink and needles, and Sabine Schanzer, Niklas Mahnke, Evelin Hagen, and Jörg Scheffel of the Charité – Universitätsmedizin Berlin for excellent technical support.

Statement of Ethics

All volunteers enrolled in the study involving intravital microscopy provided their written informed consent before participation, and a positive vote had been obtained from the Ethics Committee of the Charité – Universitätsmedizin Berlin (EA1-093-18, EA1-324-19) according to the Declaration of Helsinki (59th WMA General Assembly, Seoul, October 2008). Consent for publication has been obtained from all study participants.

Conflict of Interest Statement

The authors have no conflicts of interest to declare.

Funding Sources

Marius Kröger is thankful for a scholarship by Charité – Universitätsmedizin Berlin. The authors are thankful to the foundation of Skin Physiology for financial support.

Author Contributions

Marius Kröger planned and designed the study. Marius Kröger, Maxim E. Darvin, Johannes Schleusener, Sora Jung, Jürgen Lademann, and Martina C. Meinke conceived the experiments. Marius Kröger and Maxim E. Darvin performed the experiments. Marius Kröger, Johannes Schleusener, and Maxim E. Darvin analyzed the data. Marius Kröger, Johannes Schleusener, Sora Jung, and Maxim E. Darvin wrote the main manuscript text. All authors reviewed the manuscript.

Data Availability Statement

The datasets used and analyzed during the current study are available from the corresponding author on reasonable request. The data that support the findings of this study are not publicly available due to their containing information that could compromise the privacy of research participants but are available from the corresponding author M.E.D.

References

1 Deter-Wolf A, Robitaille B, Krutak L, Galliot S. The world's oldest tattoos. J Archaeol Sci Rep. 2016 Feb;5:19–24.
2 Regensburger J, Lehner K, Maisch T, Vasold R, Santarelli F, Engel E, et al. Tattoo inks contain polycyclic aromatic hydrocarbons that additionally generate deleterious singlet oxygen. Exp Dermatol. 2010;19(8):275–81.
3 Høgsberg T, Loeschner K, Löf D, Serup J. Tattoo inks in general usage contain nanoparticles. Br J Dermatol. 2011;165(6):1210–8.
4 Darvin ME, Schleusener J, Parenz F, Seidel O, Krafft C, Popp J, et al. Confocal Raman microscopy combined with optical clearing for identification of inks in multicolored tattooed skin: in vivo. Analyst. 2018;143(20):4990–9.
5 Tammaro A, Fatuzzo G, Narcisi A, Abruzzese C, Caperchi C, Gamba A, et al. Laser removal of tattoos. Int J Immunopathol Pharmacol. 2012;25(2):537–9.
6 Khunger N, Molpariya A, Khunger A. Complications of tattoos and tattoo removal: stop and think before you ink. J Cutan Aesthet Surg. 2015;8(1):30–6.
7 Armstrong ML, Stuppy DJ, Gabriel DC, Anderson RR. Motivation for tattoo removal. Arch Dermatol. 1996 Apr;132(4):412–6.
8 Giulbudagian M, Schreiver I, Singh AV, Laux P, Luch A. Safety of tattoos and permanent make-up: a regulatory view. Arch Toxicol. 2020;94(2):357–69.
9 von Haam E, Mallette FS. Studies on the toxicity and skin effects of compounds used in the rubber and plastics industries. III. Carcinogenicity of carbon black extracts. AMA Arch Ind Hyg Occup Med. 1952 Sep;6(3):237–42.
10 Laux P, Tralau T, Tentschert J, Blume A, Dahouk SA, Bäumler W, et al. A medical-toxicological view of tattooing. Lancet. 2016;387(10016):395–402.
11 Hutton Carlsen K, Larsen G, Serup J. Tattoo pigment agglomerates measured in commercial ink stock products by computerised light microscopy. Skin Res Technol. 2020;26(2):292–300.
12 Magrez A, Kasas S, Salicio V, Pasquier N, Seo JW, Celio M, et al. Cellular toxicity of carbon-based nanomaterials. Nano Lett. 2006;6(6):1121–5.
13 Crosera M, Bovenzi M, Maina G, Adami G, Zanette C, Florio C, et al. Nanoparticle dermal absorption and toxicity: a review of the literature. Int Arch Occup Environ Health. 2009;82(9):1043–55.
14 Pernodet N, Fang X, Sun Y, Bakhtina A, Ramakrishnan A, Sokolov J, et al. Adverse effects of citrate/gold nanoparticles on human dermal fibroblasts. Biomed Opt Express. 2006;2(6):766–73.
15 Strandt H, Voluzan O, Niedermair T, Ritter U, Thalhamer J, Malissen B, et al. Macrophages and fibroblasts differentially contribute to tattoo stability. Dermatology. 2021;237(2):296–302.
16 Pedata P, Boccellino M, La Porta R, Napolitano M, Minutolo P, Sgro LA, et al. Interaction between combustion-generated organic nanoparticles and biological systems: in vitro study of cell toxicity and apoptosis in human keratinocytes. Nanotoxicology. 2012;6(4):338–52.
17 Shvedova AA, Castranova V, Kisin ER, Schwegler-Berry D, Murray AR, Gandelsman VZ, et al. Exposure to carbon nanotube material: assessment of nanotube cytotoxicity using human keratinocyte cells. J Toxicol Environ Health A. 2003;66(20):1909–26.
18 Ling MP, Chio CP, Chou WC, Chen WY, Hsieh NH, Lin YJ, et al. Assessing the potential exposure risk and control for airborne titanium dioxide and carbon black nanoparticles in the workplace. Environ Sci Pollut Res Int. 2011;18(6):877–89.
19 Jatana S, Palmer BC, Phelan SJ, Delouise LA. Immunomodulatory effects of nanoparticles on skin allergy. Sci Rep. 2017;7(1):3979–11.
20 Yoshioka Y, Kuroda E, Hirai T, Tsutsumi Y, Ishii KJ. Allergic responses induced by the immunomodulatory effects of nanomaterials upon skin exposure. Front Immunol. 2017;8:169.
21 Lewis Pinocytosis. 1937;1(1):666–79.
22 Sterry W, Künne N, Weber-Matthiesen K, Brasch J, Mielke V. Cell trafficking in positive and negative patch-test reactions: demonstration of a stereotypic migration pathway. J Invest Dermatol. 1991 Apr;96(4):459–62.
23 Achachi A, Vocanson M, Bastien P, Péguet-Navarro J, Grande S, Goujon C, et al. UV radiation induces the epidermal recruitment of dendritic cells that compensate for the depletion of Langerhans cells in human skin. J Invest Dermatol. 2015 Aug;135(8):2058–67.
24 Willis CM, Stephens CJM, Wilkinson JD. Differential patterns of epidermal leukocyte infiltration in patch test reactions to structurally unrelated chemical irritants. J Invest Dermatol. 1993;101(3):364–70.
25 Kluger N, Koljonen V. The surgeon, the tattoo and the black lymph node. J Plast Reconstr Aesthet Surg. 2013;66(4):561–2.
26 Sepehri M, Sejersen T, Qvortrup K, Lerche CM, Serup J. Tattoo pigments are observed in the kupffer cells of the liver indicating bloodborne distribution of tattoo ink. Dermatology. 2017;233(1):86–93.
27 Baranska A, Shawket A, Jouve M, Baratin M, Malosse C, Voluzan O, et al. Unveiling skin macrophage dynamics explains both tattoo persistence and strenuous removal. J Exp Med. 2018;215(4):1115–33.
28 Van Zuijlen PPM, Ruurda JJB, Van Veen HA, Van Marle J, Van Trier AJM, Groenevelt F, et al. Collagen morphology in human skin and scar tissue: no adaptations in response to mechanical loading at joints. Burns. 2003;29(5):423–31.
29 Grant CA, Twigg PC, Baker R, Tobin DJ. Tattoo ink nanoparticles in skin tissue and fibroblasts. Beilstein J Nanotechnol. 2015;6(1):1183–91.
30 Suter MM, Schulze K, Bergman W, Welle M, Roosje P, Müller EJ. The keratinocyte in epidermal renewal and defence. Vet Dermatol. 2009;20(5–6):515–32.
31 Lea PJ, Pawlowski A. Human tattoo. Electron microscopic assessment of epidermis, epidermal-dermal junction, and dermis. Int J Dermatol. 1987;26(7):453–8.
32 Taylor CR, Anderson RR, Gange RW, Michaud NA, Flotte TJ. Light and electron microscopic analysis of tattoos treated by Q-switched ruby laser. J Invest Dermatol. 1991 Jul;97(1):131–6.
33 Milton R, Okun MR. Carbon particles in melanocytes and basal cells as a result of a tattoo. J Invest Dermatol. 1965;44(6):433–4.
34 Sperry K. Tattoos and tattooing. Part II: gross pathology, histopathology, medical complications, and applications. Am J Forensic Med Pathol. 1992 Mar;13(1):7–17.
35 Høgsberg T, Thomsen BM, Serup J. Histopathology and immune histochemistry of red tattoo reactions: interface dermatitis is the lead pathology, with increase in T-lymphocytes and Langerhans cells suggesting an allergic pathomechanism. Skin Res Technol. 2015;21(4):449–58.
36 Shah H, Tivary AK, Kumar P. Transepidermal elimination: historical evolution, pathogenesis and nosology hiral. Indian J Dermatol Venereol Leprol. 2018;84(1):6–15.
37 Bayoumi AHM, Marks R. Transepidermal elimination: studies with an animal model. Br J Exp Pathol. 1980;61(6):560–6.
38 Woo TY, Rasmussen JE. Disorders of transepidermal elimination: part 2. Int J Dermatol. 1985;24(6):337–48.

39 Schreiver I, Hesse B, Seim C, Castillo-Michel H, Anklamm L, Villanova J, et al. Distribution of nickel and chromium containing particles from tattoo needle wear in humans and its possible impact on allergic reactions. Part Fibre Toxicol. 2019;16(1):33–10.
40 Ando H, Niki Y, Ito M, Akiyama K, Matsui MS, Yarosh DB, et al. Melanosomes are transferred from melanocytes to keratinocytes through the processes of packaging, release, uptake, and dispersion. J Invest Dermatol. 2012;132(4):1222–9.
41 Yakimov BP, Shirshin EA, Schleusener J, Allenova AS, Fadeev VV, Darvin ME. Melanin distribution from the dermal: epidermal junction to the stratum corneum–non-invasive in vivo assessment by fluorescence and Raman microspectroscopy. Sci Rep. 2020;10(1):14374.
42 Hurbain I, Romao M, Sextius P, Bourreau E, Marchal C, Bernerd F, et al. Melanosome distribution in keratinocytes in different skin types: melanosome clusters are not degradative organelles. J Invest Dermatol. 2018; 138(3):647–56.
43 Brady BG, Gold H, Leger EA, Leger MC. Self-reported adverse tattoo reactions: a New York City Central Park study. Contact Dermatitis. 2015;73(2):91–9.
44 Islam PS, Chang C, Selmi C, Generali E, Huntley A, Teuber SS, et al. Medical complications of tattoos: a comprehensive review. Clin Rev Allergy Immunol. 2016;50(2): 273–86.
45 König K. Clinical multiphoton tomography. J Biophotonics. 2008;1(1):13–23.
46 Darvin ME, Richter H, Zhu YJ, Meinke MC, Knorr F, Gonchukov SA, et al. Comparison of in vivo and ex vivo laser scanning microscopy and multiphoton tomography application for human and porcine skin imaging. Quan Electron. 2014;44(7):646–51.
47 Ulrich M, Klemp M, Darvin ME, König K, Lademann J, Meinke MC. In vivo detection of basal cell carcinoma: comparison of a reflectance confocal microscope and a multiphoton tomograph. J Biomed Opt. 2013; 18(6):061229.
48 Kröger M, Scheffel J, Shirshin EA, Schleusener J, Meinke MC, Lademann J, et al. Label-free imaging of macrophage phenotypes and phagocytic activity in the human dermis in vivo using two-photon excited FLIM. bioRxiv. 2021 Jan:470361.
49 Kröger M, Scheffel J, Nikolaev VV, Shirshin EA, Siebenhaar F, Schleusener J, et al. In vivo non-invasive staining-free visualization of dermal mast cells in healthy, allergy and mastocytosis humans using two-photon fluorescence lifetime imaging. Sci Rep. 2020;10(1):14930.
50 Shirshin EA, Gurfinkel YI, Priezzhev AV, Fadeev VV, Lademann J, Darvin ME. Two-photon autofluorescence lifetime imaging of human skin papillary dermis in vivo: assessment of blood capillaries and structural proteins localization. Sci Rep. 2017;7(1):1171.
51 Kröger M, Schleusener J, Jung S, Darvin ME. Characterization of collagen I fiber thickness, density, and orientation in the human skin in vivo using second-harmonic generation imaging. Photonics. 2021 Sep;8(9):404.
52 Babina M, Guhl S, Stärke A, Kirchhof L, Zuberbier T, Henz BM. Comparative cytokine profile of human skin mast cells from two compartments-strong resemblance with monocytes at baseline but induction of IL-5 by IL-4 priming. J Leukoc Biol. 2004;75(2): 244–52.
53 Rittié L, Fisher GJ. Isolation and culture of skin fibroblasts. In: Varga J, Brenner DA, Phan SH, editors. Fibrosis research: methods and protocols. Totowa (NJ): Humana Press; 2005. p. 83–98.
54 Fitzpatrick TB. The validity and practicality of sun-reactive skin types I through VI. Arch Dermatol. 1988;124(6):869–71.
55 Weinigel M, Breunig HG, Kellner-Höfer M, Bückle R, Darvin ME, Klemp M, et al. In vivo histology: optical biopsies with chemical contrast using clinical multiphoton/coherent anti-Stokes Raman scattering tomography. Laser Phys Lett. 2014;11(5):055601.
56 Zhu Y, Choe C-S, Ahlberg S, Meinke MC, Alexiev U, Lademann J, et al. Penetration of silver nanoparticles into porcine skin ex vivo using fluorescence lifetime imaging microscopy, Raman microscopy, and surface-enhanced Raman scattering microscopy. J Biomed Opt. 2015;20(5):051006.
57 Petersen H, Roth K. Vom pigment zum porträt. Chem Unserer Zeit. 2016;50(1):44–6.
58 Molina N, Aguirre J, Walczak M. Application of FFT analysis for the study of directionality of wear scars in exposure to slurry flow of varying velocity. Wear. 2019;426–427: 589–95.
59 Yakimov BP, Gogoleva MA, Semenov AN, Rodionov SA, Novoselova MV, Gayer AV, et al. Label-free characterization of white blood cells using fluorescence lifetime imaging and flow-cytometry: molecular heterogeneity and erythrophagocytosis [Invited]. Biomed Opt Express. 2019;10(8):4220–36.
60 Zonios G, Dimou A, Bassukas I, Galaris D, Tsolakidis A, Kaxiras E. Melanin absorption spectroscopy: new method for noninvasive skin investigation and melanoma detection. J Biomed Opt. 2008;13(1):014017.
61 Büngeler A, Hämisch B, Strube OI. The supramolecular buildup of eumelanin: structures, mechanisms, controllability. Int J Mol Sci. 2017;18(9):1901.
62 Baroni A, Buommino E, De Gregorio V, Ruocco E, Ruocco V, Wolf R. Structure and function of the epidermis related to barrier properties. Clin Dermatol. 2012;30(3):257–62.
63 Mulholland WJ, Arbuthnott EAH, Bellhouse BJ, Cornhill JF, Austyn JM, Kendall MAF, et al. Multiphoton high-resolution 3D imaging of Langerhans cells and keratinocytes in the mouse skin model adopted for epidermal powdered immunization. J Invest Dermatol. 2006;126(7):1541–8.
64 Tong PL, Roediger B, Kolesnikoff N, Biro M, Tay SS, Jain R, et al. The skin immune atlas: three-dimensional analysis of cutaneous leukocyte subsets by multiphoton microscopy. J Invest Dermatol. 2015;135(1):84–93.
65 Morhenn VB, Lemperle G, Gallo RL. Phagocytosis of different particulate dermal filler substances by human macrophages and skin cells. Dermatol Surg. 2002;28(6):484–90.
66 Serup J, Carlsen KH, Sepehri M. Tattoo complaints and complications: diagnosis and clinical spectrum. Curr Probl Dermatol. 2015; 48:48–60.
67 Bäumler W. Tätowierungen und mögliche gesundheitliche Folgen. Dtsch Arztebl Int. 2016;113(40):663–4.
68 Rasmussen S, O'Connor RC. Factors influencing anticipated decisions about sunscreen use. J Health Psychol. 2005;10(4):585–95.
69 Jovanovic Z, Schornstein T, Sutor A, Neufang G, Hagens R. Conventional sunscreen application does not lead to sufficient body coverage. Int J Cosmet Sci. 2017;39(5):550–5.
70 Proksch E, Brasch J, Sterry W. Integrity of the permeability barrier regulates epidermal Langerhans cell density. Br J Dermatol. 1996; 134(4):630–8.
71 Kang K, Hammerberg C, Maunier L, Cooper KD. CD11b+ macrophages that infiltrate human epidermis after in vivo ultraviolet exposure potently produce IL-10 and represent the major secretory source of epidermal IL-10. J Immunol. 2016.
72 Meunier L, Bata-Csorgo Z, Cooper KD. In human dermis, ultraviolet radiation induces expansion of a CD36+ CD11b+ CD1- macrophage subset by infiltration and proliferation; CD1+ Langerhans-like dendritic antigen-presenting cells are concomitantly depleted. J Invest Dermatol. 1995;105(6):782–8.
73 Steigbigel RT, Lambert LH, Remington JS. Phagocytic and bacterial properties of normal human monocytes. J Clin Invest. 1974;53(1): 131–42.
74 Gu BJ, Sun C, Fuller S, Skarratt KK, Petrou S, Wiley JS. A quantitative method for measuring innate phagocytosis by human monocytes using real-time flow cytometry. Cytometry A. 2014;85(4):313–21.
75 Fernando IPS, Kim HS, Sanjeewa KKA, Oh JY, Jeon YJ, Lee WW. Inhibition of inflammatory responses elicited by urban fine dust particles in keratinocytes and macrophages by diphlorethohydroxy-carmalol isolated from a brown alga ishige okamurae. Algae. 2017;32(3):261–73.
76 Ferguson JE, Andrew SM, Jones CJP, August PJ. The Q-switched neodymium: YAG laser and tattoos–a microscopic analysis of laser-tattoo interactions. Br J Dermatol. 1997;137(3):405–10.
77 Fujita H, Nishii Y, Yamashita K, Kawamata S, Yoshikawa K. The uptake and long-term storage of India ink particles and latex beads by fibroblasts in the dermis and subcutis of mice, with special regard to the non-inflammatory defense reaction by fibroblasts. Arch Histol Cytol. 1988;51(3):285–94.

78 Abdel-Fattah NS, El-Kahky H, El-Badawy N, Ël-Gothamy Z. Medical Tattoos. J Egypt Women's Dermatol Soc. 2004;1(1):25–33.
79 Falconi M, Teti G, Zago M, Galanzi A, Breschi L, Pelotti S, et al. Influence of a commercial tattoo ink on protein production in human fibroblasts. Arch Dermatol Res. 2009;301(7):539–47.
80 Kawaguchi Y, Tanaka H, Okada T, Konishi H, Takahashi M, Ito M, et al. Effect of reactive oxygen species on the elastin mRNA expression in cultured human dermal fibroblasts. Free Radic Biol Med. 1997;23(1):162–5.
81 Mostaço-Guidolin L, Rosin NL, Hackett TL. Imaging collagen in scar tissue: developments in second harmonic generation microscopy for biomedical applications. Int J Mol Sci. 2017;18(8):1772.
82 Pittet J-CC, Freis O, Vazquez-Duchêne M-DD, Périé G, Pauly G. Evaluation of elastin/collagen content in human dermis in-vivo by multiphoton tomography-variation with depth and correlation with aging. Cosmetics. 2014;1(3):211–21.
83 Engel E, Santarelli F, Vasold R, Maisch T, Ulrich H, Prantl L, et al. Modern tattoos cause high concentrations of hazardous pigments in skin. Contact Dermatitis. 2008;58(4):228–33.